Cardiovascular Drugs and Therapy (2023) 37:891–904
https://doi.org/10.1007/s10557-022-07339-7

ORIGINAL ARTICLE

Mesenchymal Stem Cell–Originated Exosomal Lnc A2M-AS1 Alleviates Hypoxia/Reperfusion-Induced Apoptosis and Oxidative Stress in Cardiomyocytes

Hang Yu[1] · Yuxiang Pan[2] · Mingming Dai[3] · Xiaoqi Wang[4] · Haibo Chen[5]

Accepted: 22 April 2022 / Published online: 11 May 2022

Abstract

Background Mesenchymal stem cell (MSC)-derived exosomes play significant roles in ameliorating cardiac damage after myocardial ischemia-reperfusion (I/R) injury. Long non-coding RNA alpha-2-macroglobulin antisense RNA 1 (Lnc A2M-AS1) was found that might protect against myocardial I/R. However, whether Lnc A2M-AS1 delivery via MSC-derived exosomes could also regulate myocardial I/R injury remains unknown.

Methods Exosomes were isolated by ultracentrifugation, and qualified by transmission electron microscopy (TEM), nanoparticle tracking analysis (NTA), and Western blot. Hypoxia/reoxygenation (H/R) treatment in human cardiomyocytes was used to mimic the process of myocardial I/R in vitro. The viability and apoptosis of cardiomyocytes were detected using cell counting kit-8, flow cytometry, and Western blot assays. The contents of lactate dehydrogenase (LDH), malondialdehyde (MDA), and superoxide dismutase (SOD) were evaluated using corresponding commercial kits. The quantitative real-time polymerase chain reaction and Western blot were used to determine the expression levels of Lnc A2M-AS1, microRNA (miR)-556-5p, and X-linked inhibitor of apoptosis protein (XIAP). The binding interaction between miR-556-5p and Lnc A2M-AS1 or XIAP was confirmed by the dual-luciferase reporter, RIP and pull-down assays.

Results Exosomes isolated from hMSCs (hMSCs-exo) attenuated H/R-induced apoptosis and oxidative stress in cardiomyocytes. Lnc A2M-AS1 was lowly expressed in AMI patients and H/R-induced cardiomyocytes. Besides, Lnc A2M-AS1 was detectable in hMSCs-exo, exosomes derived from Lnc A2M-AS1-transfected hMSCs weakened H/R-induced apoptosis and oxidative stress, and enhanced the protective action of hMSCs-exo on H/R-induced cardiomyocytes. Further mechanism analysis showed that Lnc A2M-AS1 acted as a sponge for miR-556-5p to increase XIAP expression level. Importantly, miR-556-5p overexpression or XIAP knockdown reversed the action of exosomal Lnc A2M-AS1 on H/R-induced cardiomyocytes.

Conclusion Lnc A2M-AS1 delivery via MSC-derived exosomes ameliorated H/R-induced cardiomyocyte apoptosis and oxidative stress via regulating miR-556-5p/XIAP, opening a new window into the pathogenesis of myocardial I/R injury.

Keywords AMI · Lnc A2M-AS1 · miR-556-5p · XIAP · Mesenchymal stem cells · Exosomes

Hang Yu and Yuxiang Pan contributed equally to this work.

✉ Xiaoqi Wang
WangXiaoqi767@163.com

✉ Haibo Chen
chenhaibo2767@163.com

[1] Department of Cardiovascular Surgery Intensive Care Unit, The Second Affiliated Hospital of Hainan Medical College, Haikou City, Hainan Province, China

[2] Department of Critical Care Medicine, The Second Affiliated Hospital of Hainan Medical College, Haikou City, Hainan Province, China

[3] Department of Neurology Three Areas, The Second Affiliated Hospital of Hainan Medical College, Haikou City, Hainan Province, China

[4] Department of Cardiovascular Surgery, The Second Affiliated Hospital of Hainan Medical College, No. 368 Yehai Avenue, Longhua District, Haikou City 570105, Hainan Province, China

[5] Department of Blood Transfusion, The Second Affiliated Hospital of Hainan Medical College, No. 368 Yehai Avenue, Longhua District, Haikou City 570105, Hainan Province, China

Introduction

Acute myocardial infarction (AMI) is one of the leading causes of the mortality of cardiovascular diseases [1]. Pathologically, AMI results from the occlusion of coronary artery, and timely and effective reperfusion of blood to the ischemic myocardium remains the only therapeutic approach for the salvage of viable ischemic myocardium and the limitation of myocardial infarction size [2]. Nevertheless, the restoration of blood supply to ischemic heart can aggravate the injury of ischemic myocardium, thus leading to ischemia-reperfusion (I/R) injury [3, 4], and cardiomyocyte death and oxidative stress have been revealed to be involved in this complex, multifactorial process [3, 5, 6].

Mesenchymal stem cells (MSCs) are multipotent stem cells with the ability for self-renewal and differentiation into tissue-specific cells such as bone, cartilage cells, cardiomyocytes, and vascular endothelial cells [7, 8]. They hold great potential for cellular therapy and regenerative medicine due to the role of MSCs in tissue wound healing, growth, and maintenance of the cell supply to compensate for cell loss owing to pathology, and apoptosis has been widely accepted [9]. Importantly, numerous studies show that MSCs can be of great significance for the regeneration of ischemic cardiac muscle [10, 11]. MSCs can produce abundant amounts of exosomes [12]. Exosomes are described as the 40–150-nm diameter vesicles, which are actively secreted from different mammalian cell types [13]. They are natural information carriers, delivering exosomal surface proteins and complex bio-functional cargoes, including lipids, proteins, nucleic acids, and other metabolites, to cells in local environments or distant metastatic sites, thus affecting the physiological and pathological behaviors of recipient cells [14–17]. Recently, plenty of evidence has shown that exosomes have protective roles in ischemic heart disease by alleviating myocardial I/R injury, promoting cardiac regeneration and angiogenesis, as well as suppressing fibrosis [18, 19]. Furthermore, MSC-derived exosomes emerge as significant players in ameliorating cardiac damage after MI and myocardial I/R injury [20, 21].

Long non-coding RNAs (lncRNAs) have been revealed to participate in diverse pathological and physiological processes, and their abnormalities in expression participated in myocardial I/R injury [22, 23]. Previous studies exhibited that lncRNA alpha-2-macroglobulin antisense RNA 1 (Lnc A2M-AS1) was decreased in MI [24]; re-expression of Lnc A2M-AS1 could notably weaken hypoxia/reoxygenation (H/R)-induced apoptosis in cardiomyocytes by regulating IL1R2 expression [25], suggesting the potential involvement of Lnc A2M-AS1 in attenuating myocardial I/R injury. In recent, a theory called the competing endogenous RNA (ceRNA) hypothesis exhibits that lncRNAs, mRNAs, and pseudogenes can regulate the expression of each other via competing for shared microRNAs (miRNA/miR), which has been clarified to be a common mechanism by which lncRNA function [26, 27]. However, the miRNA/mRNA axis underlying Lnc A2M-AS1 in myocardial I/R injury is still vague. Besides that, Lnc A2M-AS1 was found to be down-regulated in exosomes derived from hypoxic cardiomyocytes [28]. However, if Lnc A2M-AS1 delivered via MSC-derived exosomes could also regulate myocardial I/R injury remains unknown.

Herein, the present work employed H/R-treated human cardiomyocytes to mimic the process of myocardial I/R in vitro to investigate whether and how exosomal Lnc A2M-AS1 from MSCs regulated H/R-mediated cardiomyocyte damage; moreover, the underlying miRNA/mRNA axis mediated the effects of Lnc A2M-AS1 was also investigated.

Materials and Methods

Patients and Blood Collection

Seventy blood samples (5 mL), including 30 health individuals without myocardial disease and 40 AMI cases, were collected from The Second Affiliated Hospital of Hainan Medical College. Following centrifugation at 2000 g for 10 min, the blood samples were preserved at −80 °C for further analysis. All AMI diagnoses were confirmed by two cardiologists. The smoking and drinking diabetic patients were excluded. This work was endorsed and supervised by the Ethics Committee of the Second Affiliated Hospital of Hainan Medical College according to the Declaration of Helsinki, and each subject provided written informed consent before this study. The detail clinical information of all subjects is shown in Table 1.

Cell Culture

Human bone marrow–derived MSCs (hMSCs) and human cardiomyocyte cell line AC16 were obtained from Jining Cell Culture Center (Shanghai, China). The hMSCs were grown in the α-modified Eagle's medium (MEM), and AC16 cells were cultured in Dulbecco's modified Eagle medium/nutrient mixture F-12 (DMEM/F-12; Life Technologies, Scotland, UK). All mediums contained 10% fetal bovine serum (FBS; HyClone, Logan, Utah, USA), 100 μg/mL streptomycin (HyClone), and 100 U/mL penicillin (HyClone), and then were maintained in 5% CO_2 atmosphere at 37 °C. Cells passaged passage 2 and 3 were used for further experiments.

Table 1 Baseline characteristics

Variables	Health control ($n = 30$)	AMI ($n = 40$)	P-value
Age, years	55.70 ± 9.60	57.50 ± 8.21	0.412
Female, % (n)	15 (50%)	22(55%)	0.678
Systolic BP (mm Hg)	129.20 ± 18.06	131.00 ± 22.60	0.712
Diastolic BP (mm Hg)	80.60 ± 9.62	79.86 ± 10.67	0.762
TC, mmol/L	4.30 ± 1.06	6.30 ± 0.62	0.000*
TG, mmol/L	1.58 ± 1.12	1.88 ± 1.36	0.316
HDL-C, mmol/L	1.03 ± 0.36	1.25 ± 0.39	0.017*
LDL-C, mmol/L	2.72 ± 0.85	2.64 ± 0.87	0.70

Values were presented as mean ± SD or n (%). Student' s t-test and χ^2 test was used respectively. $P < 0.05$ was considered significant

Abbreviations: *HDL-C* high-density lipoprotein cholesterol, *LDL-C* low-density lipoprotein cholesterol, *TC* total cholesterol, *TG* triglycerides

Isolation and Identification of Exosome

The isolation of exosomes prepared from hMSCs as previously described [29]. Following 48 h of culture, the exosome-depleted conditioned culture medium of hMSCs was collected and centrifuged at 4000 × g for 10 min at 4 °C to remove cell fragments, followed by centrifugation at 17,000 × g for 1 h at 4 °C to remove remaining macropolymers. After filtering with a 0.22-μm pore filter, the filtrate was further ultracentrifuged at 200,000 × g for 1 h at 4 °C. Then, vesicles were collected, resuspended in phosphate-buffered saline (PBS), and repeatedly subjected to a ultracentrifugation at 200,000 × g for 1 h at 4 °C; then, exosomes were collected and dissolved in ice-cold PBS for further analysis. The structures of exosomes were identified by the transmission electron microscopy (TEM) (FEI, Hillsboro, OR, USA) (× 200), and nanoparticle tracking analysis (NTA) (NanoSight NS300, Malvern Panalytical, Malvern, UK) was performed to quality the size distribution of exosomes. For cell incubation, AC16 cells (2×10^5) were co-cultured with 10 μg exosomes of each group for 48 h.

Cell Transfection

For transient transfection, hMSCs (5×10^5) or AC16 cells (1×10^6) were plated at a dish until 80% confluence. 2 μg of pcDNA3.1-Lnc A2M-AS1 overexpressing plasmid (Lnc A2M-AS1) or negative control (vector) (GeneCopoepia Biosciences, Shanghai, China) were transfected into hMSCs. Besides, 50 nM of miR-556-5p mimic (miR-556-5p), 50 nM of XIAP small interfering RNA (siRNA) (si-XIAP), or the negative control (miR-NC or si-NC) (GeneCopoepia Biosciences) were transfected into AC16 cells, followed by co-culturing with indicated exosomes. 50 nM of miR-556-5p inhibitor or negative control (anti-miR-NC) were transfected into AC16 cells. All transfection was conducted using the Lipofectamine 2000 (Invitrogen, San Diego, CA, USA) according to the manufacturer's protocol.

H/R Simulation

AC16 cells were cultivated in a hypoxic chamber at 37 °C with serum- and glucose-deficient DMEM/F-12 for 6 h, followed by reoxygenation for 12 h in DMEM/F12 containing 10% FBS with 5% CO_2 and 95% air at 37 °C. Cells cultured under normal oxygen conditions were used as the control.

Cell Counting Kit-8 Assay

AC16 cells were plated into each well of 96-well plates for 48 h. Then, cell viability was assayed using the CCK-8 solution (10 μL, Biotech, Nanjing, China) by reading absorbance at 450 nm with a microplate reader.

Flow Cytometer

Cell apoptosis was analyzed by the staining of Annexin V labeled by fluorescein isothiocvanate (FITC) (10 μL, BD Biosciences, Heidelberg, Germany) and propidium iodide (PI) (10 μL; Life Technologies) under darkness using a FACSCalibur flow cytometry (BD Biosciences).

Western Blot

AC16 cells and exosomes were homogenized in RIPA lysis buffer; then, protein was separated by 10% SDS-polyacrylamide gel electrophoresis and transferred onto a nitrocellulose membrane. After with 5% non-fat milk blocking for 1 h, the membrane was incubated with primary antibodies at 4 °C all might, followed by probing with secondary antibody at 37 °C for 2 h. Membranes carrying protein blots were visualized by ECL detection system (Life Technologies). The primary antibodies included TSG101 (1:5000, ab125011), CD81 (1: 2000, ab109201), CD63 (1:2000, ab68418), CD9 (1:2000, ab92726), Calnexin (1:2000, ab22595) B-cell lymphoma-2 (Bcl-2) (1:1000, ab692), Bcl-2-associated X protein (Bax) (1:1000, ab32503), Cleaved-caspase 3 (c-caspase 3) (ab2302, Abcam), caspase 3 (1:5000, ab32351), and glyceraldehyde-phosphate dehydrogenase (GAPDH) (1:5000, ab181602) (Abcam, Cambridge, MA, USA).

Measurement of Lactate Dehydrogenase, Malondialdehyde, and Superoxide Dismutase

AC16 cells were centrifuged at 4000 g for 10 min at 37 °C; then, the resulting supernatant was collected and commercial LDH, MDA, and SOD determination kits obtained from Sangon Biotech (Shanghai, China) were used to measure their contents referring to the manufacturer's recommendations.

Quantitative Real-Time Polymerase Chain Reaction

Total RNA was isolated from blood samples, cultured cells, and exosomes using trizol reagent (Life Technologies). Reverse transcription was performed from 1 μg of RNA using the PrimeScript RT Reagent Kit (Takara, Dalian, China). Levels of mRNAs and miRNAs were quantified by quantitative real-time PCR with SYBR® Select Master Mix (Takara). U6 or GAPDH was used as the normalization control. The primer sequences were listed as follows:

Lnc A2M-AS1: F 5′-GCACCACACAGAAGTGATAGC-3′, R 5′-TGAGCCAAGAGAGTCTGAGGA-3′;
X-linked inhibitor of apoptosis protein (XIAP): F 5′-ACC GTGCGGTGCTTTAGTT-3′, R 5′-TGCGTGGCACTA TTTTCAAGATA-3′;
GAPDH: miR-556-5p: F 5′-GGCAGGGATGAGCTC ATTGTA-3′, R 5′-CTCAACTGGTGTCGTGGA-3′;
U6: F 5′-CTCGCTTCGGCAGCACA-3′, R 5′-AACGCT TCACGAATTTGCGT-3′.

Dual-Luciferase Reporter Assay

The direct relations between miR-556-5p and Lnc A2M-AS1 or XIAP 3′ untranslated region (3′UTR) were estimated by bioinformatics analysis. The Lnc A2M-AS1 or XIAP wild (WT) and mutant (MUT) sequences produced by GenePharma (Shanghai, China) were inserted into the pGL3-Basic Vector to establish luciferase reporter vectors (Lnc A2M-AS1-WT/MUT or XIAP 3′ UTR-WT/MUT). HEK293 cells (Jining Cell Culture Center, Shanghai, China) infected with miR-556-5p mimic or mimic control were seeded into 96-well plates. When the cell density reached 70% confluency, cells were transfect with 50 ng pGL3 Vector and 10 ng pRL-TK Renilla. Finally, the Dual-Luciferase Reporter Assay System (Promega, Madison, WI, USA) was used to determine the luciferase activity.

RNA Immunoprecipitation Assay

RIP assay was performed according to the instructions of Magna RIP RNA-Binding Protein Immunoprecipitation Kit (Millipore, Billerica, MA, USA) with antibodies specific for Argonaute 2 (Ago2) (ab186733, Abcam) or control IgG (Millipore). The coprecipitated RNAs were then eluted, used for cDNA synthesis, and detected by qRT-PCR.

Pull Down Assay

AC16 cells were lysed and then incubated with streptavidin-coated magnetic beads containing biotin-labeled miR-556-5p (Bio-miR-556-5p wt), Bio-miR-556-5p mut, or Bio-miR-NC (Life Technologies) at 4 °C overnight. After being digested by proteinase K, beads were extensively washed, and the expression of Lnc A2M-AS1 and XIAP was assayed.

Statistical Analysis

Data were displayed in the form of mean ± standard deviation (SD). Group comparison was conducted using Student's *t* test (two-sided) or analysis of variance followed by Tukey' s post hoc analysis. Pearson's correlation coefficient was applied to evaluate the relationship between two variables. Data analysis was performed using GraphPad Prism 7 software (GraphPad, San Diego, CA, USA) with $P < 0.05$ suggested statistically significant.

Results

Identification of Exosomes Isolated from hMSCs

We isolated exosomes in cultured hMSCs, named as hMSCs-exo. TEM data showed a typical cup-shaped morphology (Fig. 1A). Western blot analysis showed that the specific exosomal markers TSG101, CD63, CD81, and CD9 were evident in exosomes, while Calnexin, a negative marker, was not detectable in exosomes (Fig. 1B). In addition, the predominant size of the vesicles was 100–140 nm, consistent with the characteristic size range of exosomes (Fig. 1C).

Exosomes Isolated from hMSCs Relieved H/R-Induced Apoptosis and Oxidative Stress in Cardiomyocytes

To determine the role of hMSCs-exo in myocardial I/R injury, AC16 cells were co-cultured with exosomes (10 μg) for 48 h, followed by H/R stimulation. CCK-8 assay showed that hMSCs-exo treatment reversed H/R stimulation-induced inhibition on AC16 cell viability (Fig. 2A). Besides that, H/R stimulation led to an increase of AC16 cell apoptosis rate, accompanied by the down-regulation of Bcl-2 protein level as well as up-regulation of Bax and c-caspase 3 protein levels, while this condition was attenuated by hMSCs-exo treatment (Fig. 2B, C). In

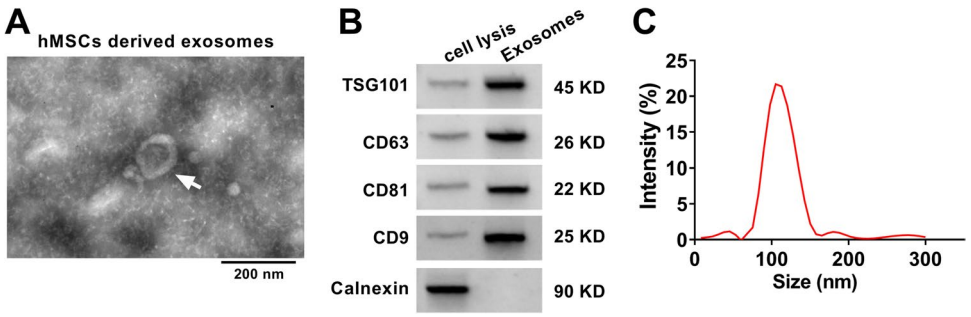

Fig. 1 Identification of exosomes isolated from hMSCs. **A** TEM images of exosomes isolated from hMSCs ($n = 3$). Scale bar, 200 nm. **B** Western blot for TSG101, CD63, CD81, and CD9 in exosomes ($n = 3$). **C** NTA for size distribution of exosomes isolated from hMSCs ($n = 3$). All experiments were repeated three times independently

addition, hMSCs-exo treatment reduced the contents of LDH and MDA, but enhanced SOD content in H/R stimulated AC16 cells, thus suppressing oxidative stress (Fig. 2D). Taken together, these results suggested that exosomes isolated from hMSCs protected cardiomyocytes against H/R injury.

Lnc A2M-AS1 Delivered via MSC-Derived Exosomes Reversed H/R-Induced Apoptosis and Oxidative Stress in Cardiomyocytes

The expression profile of Lnc A2M-AS1 was analyzed in AMI patients, and the detail clinical characteristics are shown in Table 1. Compared with health control, patients

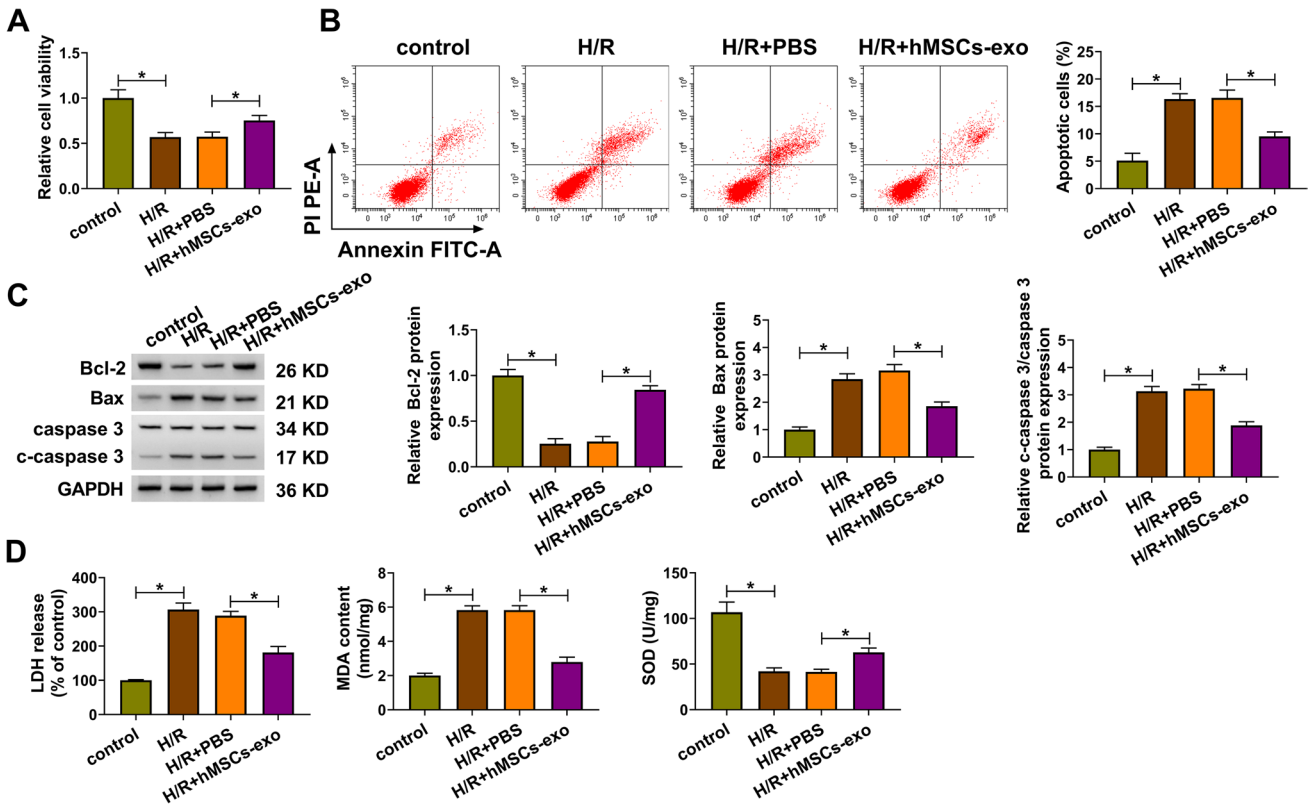

Fig. 2 Exosomes isolated from hMSCs relieved H/R-induced apoptosis and oxidative stress in cardiomyocytes. **A**–**D** AC16 cells were cultured with exosomes (10 μg) or PBS, followed by H/R stimulation. **A** CCK-8 assay for cell viability analysis ($n = 3$). **B** Flow cytometric analysis of cell apoptosis ($n = 3$). **C** Measurement of Bcl-2, Bax, caspase 3, and c-caspase 3 protein levels using Western blot ($n = 3$). **D** Detection of LDH, MDA, and SOD contents in cells using corresponding commercial kits ($n = 3$). All experiments were repeated three times independently. *$P < 0.05$

with AMI were correlated with age triglycerides (TG), and high-density lipoprotein cholesterol (HDL-C) in the serum. Moreover, compared with the healthy individuals, Lnc A2M-AS1 expression was lower in the blood samples of AMI (Fig. 3A), and there was no gender difference in term of LncA2M-AS1 expression (Fig. S1A). Consistent with the expression profile of Lnc A2M-AS1 in AMI, H/R stimulation induced a significant reduction of Lnc A2M-AS1 expression in AC16 cells (Fig. 3B). Thus, we speculated that Lnc A2M-AS1 might be associated with myocardial I/R injury. To evaluate the role of exosomal Lnc A2M-AS1 in myocardial I/R injury, hMSCs were transfected with Lnc A2M-AS1 or vector, then exosomes were isolated from transfected hMSCs. The morphology and identification of exosomes are shown in Fig. S2A, B. As expected, Lnc A2M-AS1 expression in exosomes isolated from Lnc

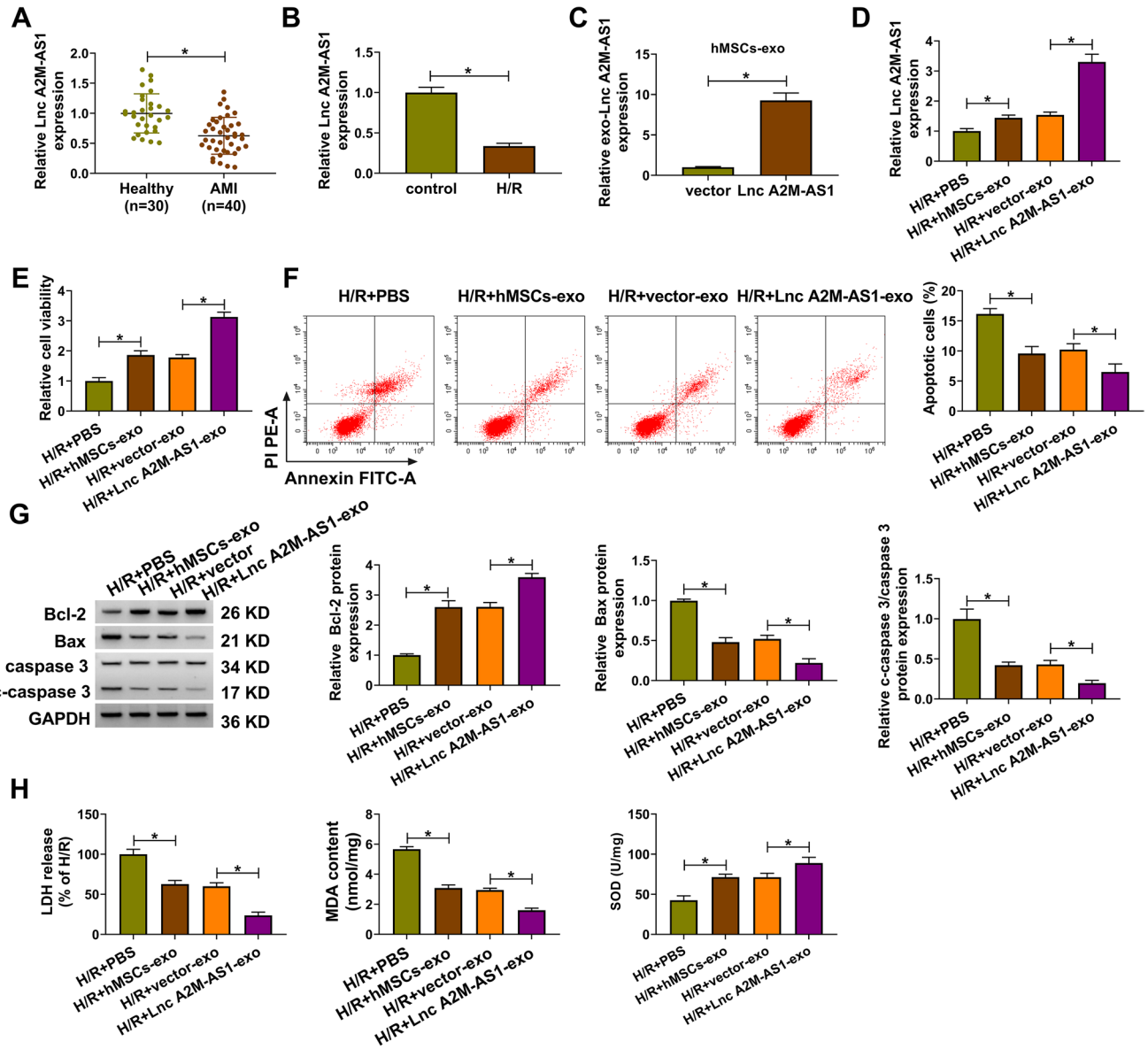

Fig. 3 Exosomes derived from Lnc A2M-AS1-transfected hMSCs transferred Lnc A2M-AS1 to cardiomyocytes and relieved H/R-induced injury. **A** The expression of Lnc A2M-AS1 was detected in AMI patients ($n = 40$) and healthy individuals ($n = 30$) using qRT-PCR. **B** Measurement of Lnc A2M-AS1 expression in AC16 cells with or without H/R stimulation was performed using qRT-PCR ($n = 3$). **C** qRT-PCR analysis of exosomal Lnc A2M-AS1 expression in exosomes isolated from hMSCs transfected with Lnc A2M-AS1 or vector ($n = 3$). **D**–**H** AC16 cells were incubated with PBS, hMSCs-exo, vector-exo, or Lnc A2M-AS1-exo, followed by H/R stimulation. **D** qRT-PCR analysis of Lnc A2M-AS1 expression in cells. **E** CCK-8 assay for cell viability analysis ($n = 3$). **F** Flow cytometric analysis of cell apoptosis ($n = 3$). **G** Western blot analysis of Bcl-2, Bax, caspase 3 and c-caspase 3 protein levels in cells ($n = 3$). **H** Measurement of LDH, MDA and SOD contents in cells using corresponding commercial kits ($n = 3$). All experiments were repeated three times independently. $^*P < 0.05$

A2M-AS1-transfected hMSCs (Lnc A2M-AS1-exo) was higher than those in exosomes isolated from vector-transfected hMSCs (vector-exo) (Fig. 3C). Then, we discovered that levels of Lnc A2M-AS1 were up-regulated in H/R-induced AC16 cells upon incubation with hMSCs-exo, and there were greater levels of Lnc A2M-AS1 in these cells exposed to Lnc A2M-AS1-exo by contrast with corresponding counterparts (Fig. 3D). Functionally, it showed that Lnc A2M-AS1-exo increased cell viability (Fig. 3E) and reduced cell apoptosis in H/R-induced AC16 cells (Fig. 3F, G). Besides, we demonstrated that Lnc A2M-AS1-exo decreased LDH and MDA levels, but increased SOD level in H/R-induced AC16 cells (Fig. 3H). These data suggested that Lnc A2M-AS1-exo secreted by hMSCs relieved H/R-induced apoptosis and oxidative stress in cardiomyocytes and enhanced the protective effects of hMSCs-exo on H/R-induced cardiomyocytes.

MiR-556-5p Was a Target of Lnc A2M-AS1

To investigate the underlying mechanism of Lnc A2M-AS1 in myocardial I/R injury, bioinformatics analysis was performed to identify miRNAs with Lnc A2M-AS1 binding sites, which showed a strong binding between Lnc A2M-AS1 and miR-556-5p (Fig. 4A). qRT-PCR analysis showed that transfection of miR-556-5p mimic significantly elevated miR-556-5p expression in HEK293T cells compared with its negative control (Fig. 4B). Then results of dual-luciferase reporter assay suggested that miR-556-5p mimic reduced the luciferase activity of the wild type Lnc A2M-AS1 vector but not the mutated one in HEK293T (Fig. 4C). Meanwhile, RIP assay showed that relative to anti-IgG immunoprecipitates, Lnc A2M-AS1 and miR-556-5p were enriched preferentially by anti-Ago2 immunoprecipitates in AC16 cells (Fig. 4D). Moreover, pull-down assay indicated that Lnc A2M-AS1 was overly captured by Bio-miR-556-5p wt in AC16 cells (Fig. 4E). All these results confirmed the direct interaction between Lnc A2M-AS1 and miR-556-5p. In addition, we up-regulated Lnc A2M-AS1 expression level in AC16 cells through the transfection of Lnc A2M-AS1 vector (Fig. 4F); it was found that Lnc A2M-AS1 overexpression reduced miR-556-5p expression level in AC16 cells (Fig. 4G). Additionally, miR-556-5p was highly expressed

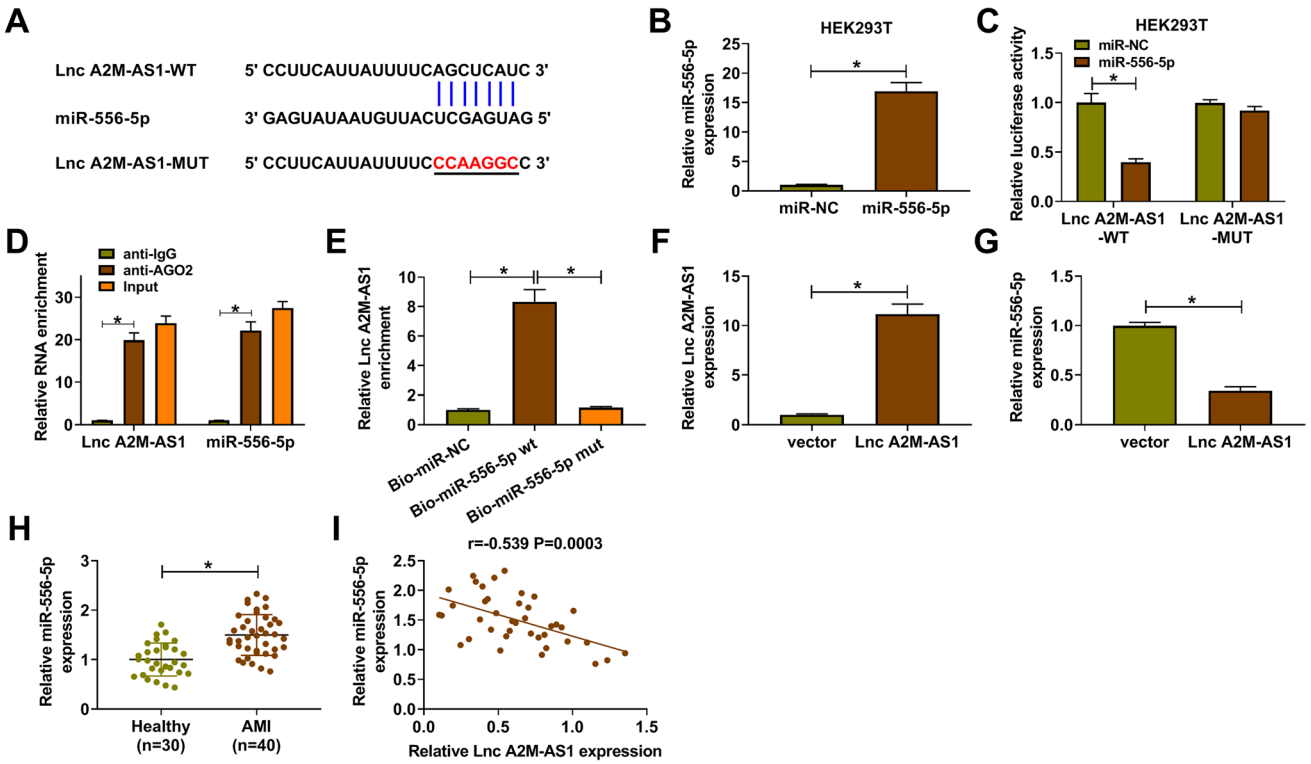

Fig. 4 MiR-556-5p was a target of Lnc A2M-AS1. **A** A putative binding site of miR-556-5p on Lnc A2M-AS1. **B** Transfection efficiency of miR-556-5p mimic in HEK293T cells using qRT-PCR ($n = 3$). **C**–**E** Interaction analysis between miR-556-5p and Lnc A2M-AS1 using dual-luciferase reporter assay, RIP assay, and pull-down assay ($n = 3$). **F**, **G** qRT-PCR of Lnc A2M-AS1 and miR-556-5p expression in AC16 cells transfected with Lnc A2M-AS1 or vector ($n = 3$). **H** Detection of miR-556-5p expression in AMI patients ($n = 40$) and healthy control ($n = 30$) using qRT-PCR. **I** Analysis of the correlation between miR-556-5p and Lnc A2M-AS1 expression using Pearson's correlation coefficient ($n = 40$). All experiments were repeated three times independently. $^*P < 0.05$

in AMI patients (Fig. 4H), which was negatively correlated with Lnc A2M-AS1 (Fig. 4I). Besides, there are no gender differences in term of miR-556-5p expression (Fig. S1B). Therefore, we confirmed that Lnc A2M-AS1 targeted miR-556-5p and suppressed its expression in cardiomyocytes.

Exosomes Derived from Lnc A2M-AS1-Transfected hMSCs Relieved H/R-Induced Injury in Cardiomyocytes Through miR-556-5p

It was discovered that miR-556-5p expression was higher in H/R-induced cardiomyocytes (Fig. 5A). Then, we analyzed whether miR-556-5p mediated the action of exosomal Lnc A2M-AS1 on H/R-induced cardiomyocytes. qRT-PCR analysis suggested that miR-556-5p mimic increased miR-556-5p level in AC16 cells (Fig. 5B). Then, transfected AC16 cells were co-cultured with Lnc

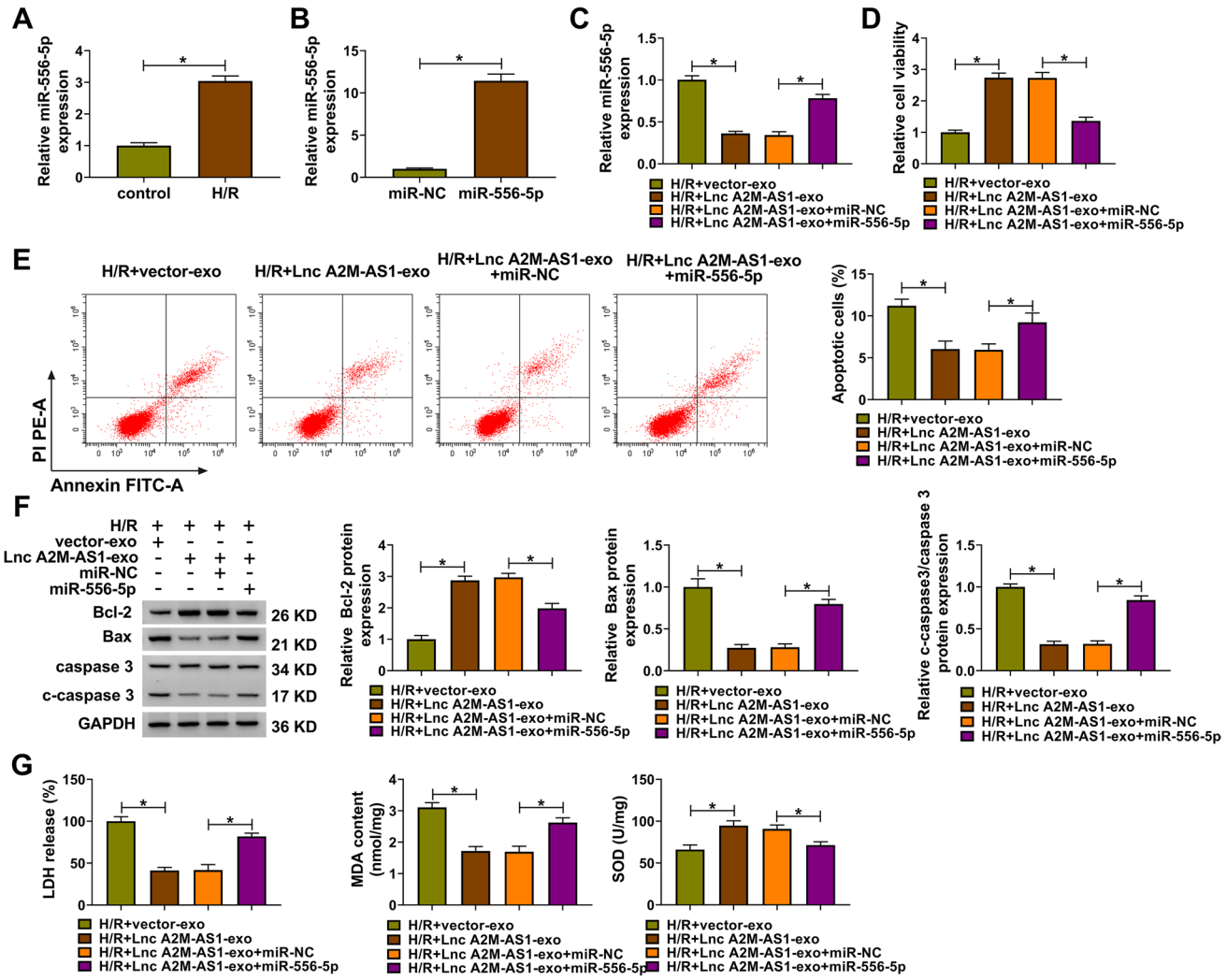

Fig. 5 Exosomes derived from Lnc A2M-AS1-transfected hMSCs attenuated H/R-induced injury in cardiomyocytes through miR-556-5p. **A** Measurement of miR-556-5p expression in AC16 cells with or without H/R stimulation using qRT-PCR ($n = 3$). **B** qRT-PCR analysis of miR-556-5p expression in AC16 cells transfected with miR-556-5p or miR-NC ($n = 3$). **C**–**G** AC16 cells were treated with vector-exo, Lnc A2M-AS1-exo, Lnc A2M-AS1-exo + miR-NC, or Lnc A2M-AS1-exo + miR-556-5p, followed by H/R stimulation. **C** qRT-PCR analysis of miR-556-5p expression in cells ($n = 3$). **D** CCK-8 assay for cell viability analysis ($n = 3$). **E** Flow cytometric analysis of cell apoptosis ($n = 3$). **F** Western blot analysis of Bcl-2, Bax, caspase 3, and c-caspase 3 protein levels in cells ($n = 3$). **G** Measurement of LDH, MDA, and SOD contents in cells using corresponding commercial kits ($n = 3$). All experiments were repeated three times independently. $^*P < 0.05$

A2M-AS1-exo; followed by H/R stimulation, it was discovered that Lnc A2M-AS1-exo down-regulated miR-556-5p expression in H/R-induced AC16 cells, which was rescued by miR-556-5p transfection (Fig. 5C). After that, rescue assay was conducted. The results showed that miR-556-5p overexpression abolished Lnc A2M-AS1-exo-evoked promotion on cell viability (Fig. 5D), suppression on cell apoptosis (Fig. 5E, F), reduction on LDH and MDA levels, and elevation on SOD content (Fig. 5G) in H/R-induced AC16 cells. In all, Lnc A2M-AS1-exo attenuated H/R-induced cardiomyocytes injury through miR-556-5p.

XIAP Was a Target of miR-556-5p and Lnc A2M-AS1 Regulated XIAP Expression by Targeting miR-556-5p

Through the starBase database, we identified XIAP as a potential target of miR-556-5p (Fig. 6A). The dual-luciferase reporter assay suggested that co-transfection of wild-type XIAP 3′UTR and a miR-556-5p mimic led to a reduction of luciferase activity in HEK293T cells (Fig. 6B). Further pull-down assay indicated that XIAP was overly captured by Bio-miR-556-5p wt in AC16 cells (Fig. 6C). Besides, we found miR-556-5p up-regulation decreased XIAP expression in AC16 cells (Fig. 6D). Furthermore, after confirming the interference efficiency of miR-556-5p inhibitor (Fig. 6E), it was observed that inhibition of miR-556-5p caused an increase of XIAP expression in AC16 cells (Fig. 6F). Therefore, we validated that miR-556-5p targeted XIAP and negatively regulated its expression. In addition, we also found Lnc A2M-AS1 elevated XIAP expression in AC16 cells (Fig. 6G), which was reduced by miR-556-5p up-regulation (Fig. 6H). Moreover, XIAP was lowly expressed in AMI patients (Fig. 6I), and there are no gender differences in XIAP expression (Fig. S1C). Besides, XIAP was negatively correlated with miR-556-5p (Fig. 6J), while positively correlated with Lnc A2M-AS1 (Fig. 6K). Thus, it was also confirmed that Lnc

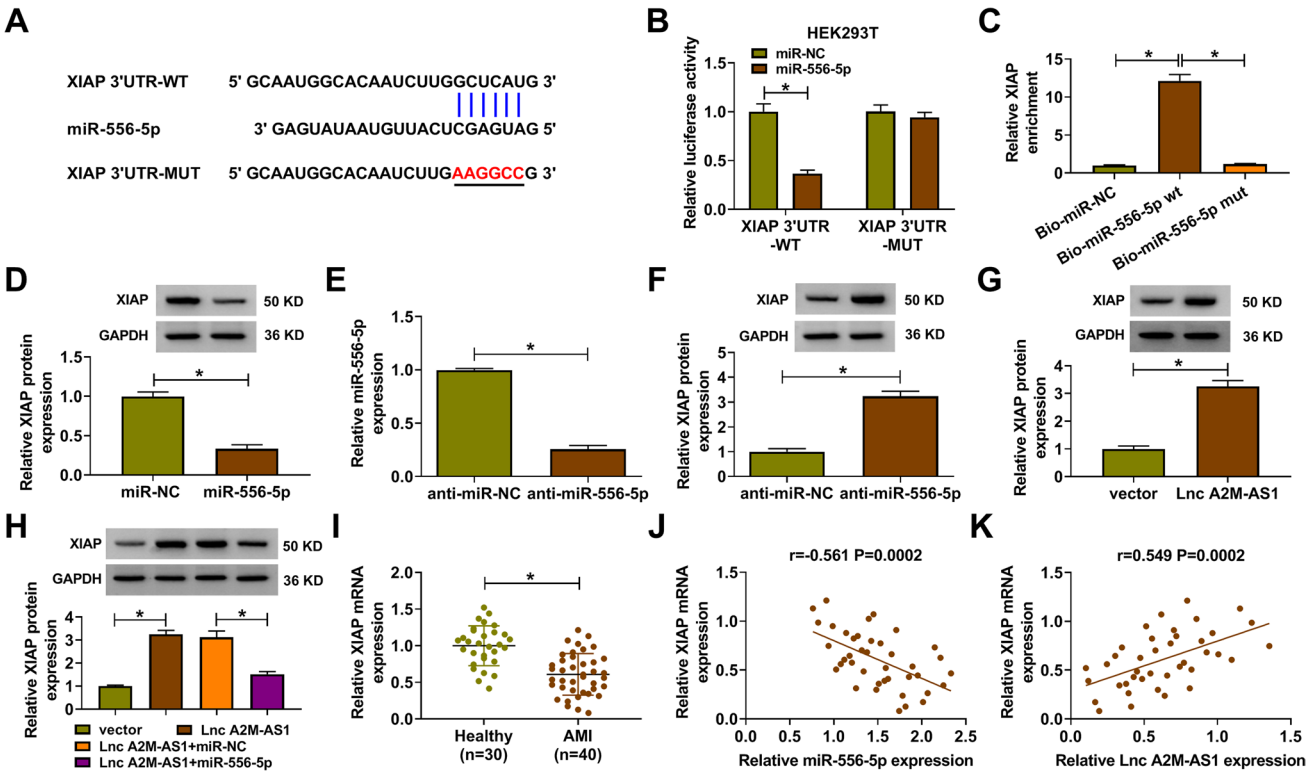

Fig. 6 XIAP was a target of miR-556-5p and Lnc A2M-AS1 regulated XIAP expression by targeting miR-556-5p. **A** A putative binding site of miR-556-5p on XIAP 3′UTR. **B**, **C** Interaction analysis between miR-556-5p and XIAP using dual-luciferase reporter assay and pull-down assay ($n = 3$). **D** Western blot analysis of XIAP level in AC16 cells transfected with miR-NC or miR-556-5p ($n = 3$). **E** qRT-PCR analysis of miR-556-5p expression in AC16 cells transfected with anti-miR-NC or anti-miR-556-5p ($n = 3$). **F** Western blot analysis of XIAP expression level in AC16 cells transfected with anti-miR-NC or anti-miR-556-5p ($n = 3$). **G** Western blot analysis of XIAP expression level in AC16 cells transfected with Lnc A2M-AS1 or vector ($n = 3$). **H** Western blot analysis of XIAP expression level in AC16 cells transfected with vector, Lnc A2M-AS1, Lnc A2M-AS1 + miR-NC, or Lnc A2M-AS1 + miR-556-5p ($n = 3$). **I** Detection of XIAP expression in AMI patients ($n = 40$) and healthy control ($n = 30$) using qRT-PCR. **J**, **K** Analysis of the correlation between XIAP and miR-556-5p or Lnc A2M-AS1 expression using Pearson's correlation coefficient ($n = 40$). All experiments were repeated three times independently. $^*P < 0.05$

A2M-AS1 served as a sponge for miR-556-5p to increase XIAP expression.

Exosomes Derived from Lnc A2M-AS1-Transfected hMSCs Attenuated H/R-Induced Cardiomyocyte Injury Through miR-556-5p

XIAP was found to be decreased by H/R stimulation in AC16 cells (Fig. 7A). Moreover, considering the Lnc A2M-AS1/miR-556-5p/XIAP axis, we further clarified whether XIAP mediated the effects of Lnc A2M-AS1-exo on H/R-induced cardiomyocytes. Western blot analysis showed that transfection of si-XIAP led to a decreased XIAP level in AC16 cells (Fig. 7B). Then transfected AC16 cells were co-cultured with Lnc A2M-AS1-exo, followed by H/R stimulation, as expected, si-XIAP transfection counteracted Lnc A2M-AS1-exo-induced elevation of XIAP expression (Fig. 7C). Functionally, XIAP knockdown attenuated Lnc A2M-AS1-exo-mediated cell viability enhancement (Fig. 7D), apoptosis reduction

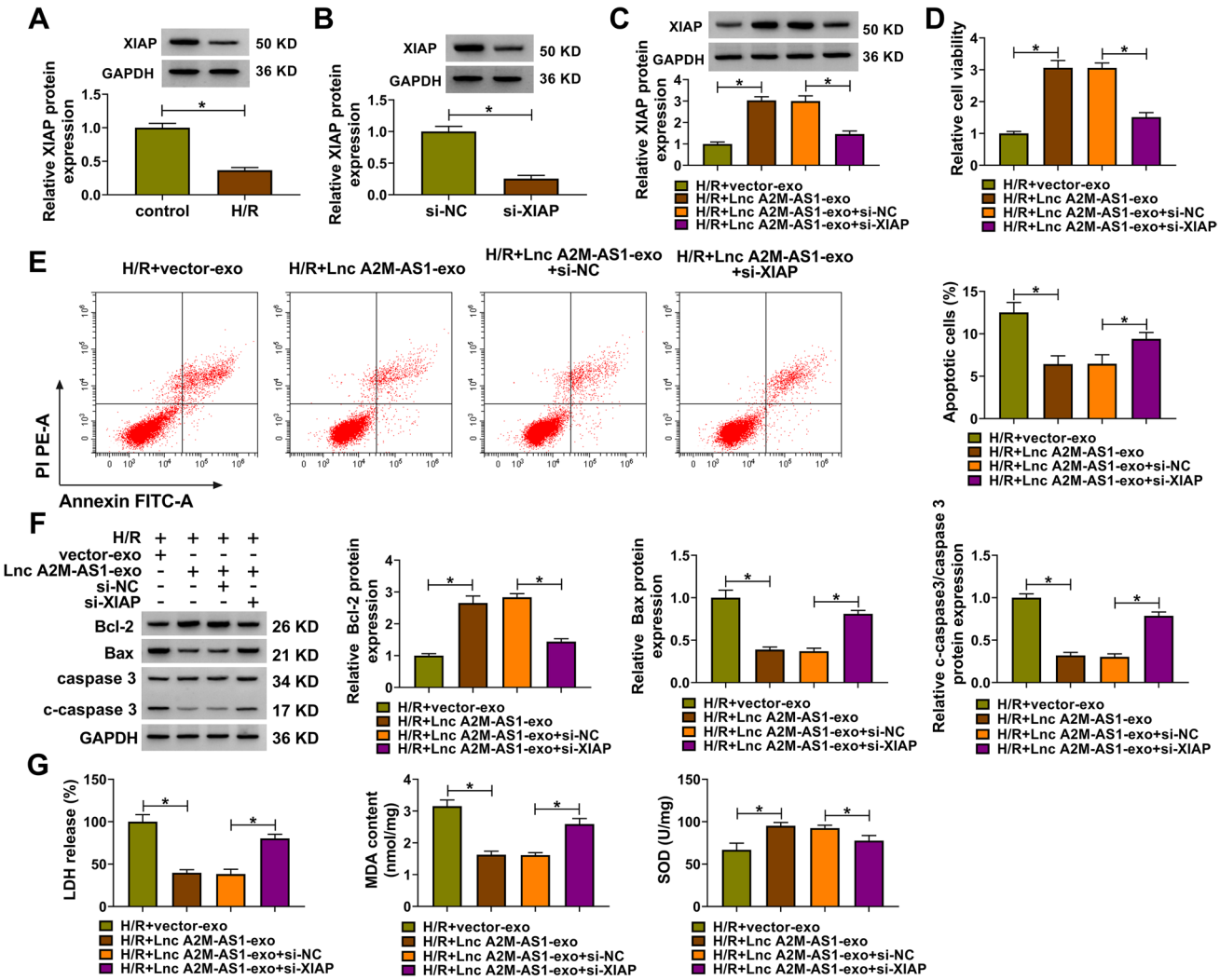

Fig. 7 Exosomes derived from Lnc A2M-AS1-transfected hMSCs reversed H/R-induced injury in cardiomyocytes through miR-556-5p. **A** Western blot analysis of XIAP expression level in AC16 cells with or without H/R stimulation ($n = 3$). **B** Detection of XIAP expression in AC16 cells transfected with si-XIAP or si-NC using Western blot ($n = 3$). **C**–**G** AC16 cells were treated with vector-exo, Lnc A2M-AS1-exo, Lnc A2M-AS1-exo + si-NC, or Lnc A2M-AS1-exo + si-XIAP, followed by H/R stimulation. **C** Western blot analysis of XIAP expression in cells. **D** CCK-8 assay for cell viability analysis ($n = 3$). **E** Flow cytometric analysis of cell apoptosis ($n = 3$). **F** Western blot analysis of Bcl-2, Bax, caspase 3, and c-caspase 3 protein levels in cells ($n = 3$). **G** Measurement of LDH, MDA and SOD contents in cells using corresponding commercial kits ($n = 3$). All experiments were repeated three times independently. $^*P < 0.05$

(Fig. 7E, F), and oxidative stress suppression (Fig. 7G). Collectively, Lnc A2M-AS1-exo protected cardiomyocytes from H/R-induced injury via XIAP.

Discussion

Recently, the use of MSCs in treating cardiovascular diseases has attracted great research interest. MSCs can secret a large number of soluble factors acting in a paracrine fashion, thus facilitating cardiomyocyte proliferation, reducing apoptosis, improving the ischaemic microenvironment and mobilizing endogenous cardiac stem cells [30]. However, researches have shown exogenous MSCs have a lower survival rate in the infarcted area despite the preferential homing of MSC to the site of myocardial ischemia [31, 32]. MSCs also can secret exosomes, which mediate intercellular communication between cells through the horizontal transfer of biologically active RNA molecules and protein [14–17]. MSC-derived exosomes were shown to rescue myocardial I/R injury by reducing cardiomyoblasts apoptosis, autophagy, or oxidative stress [20, 33]. Importantly, exosomes are stably presented in body fluids, not at risk of aneuploidy, and do not elicit adverse immune responses [20]. Therefore, MSC-derived exosomes are considered to be ideal drug delivery vehicles.

In this study, we demonstrated that MSC-derived exosomes enhanced viability and reduced apoptosis in H/R-damaged cardiomyocytes in vitro. Besides that, we also detected a decrease in the activity of MDA and LDH, and an increase in SOD content after the administration of MSC-derived exosomes in H/R-damaged cardiomyocytes, suggesting the suppression of myocardial injury and oxidative stress. This study confirmed that MSC-derived exosomes have beneficial effects on H/R-induced cardiomyocytes in vitro. However, the underlying mechanism is still vague. Exosomes usually exert their action through delivering cargo, which include lncRNAs [34]. LncRNAs are a kind of transcripts longer than 200 bp and mostly lack without protein-coding capacity. Many scholars have revealed that lncRNAs play an important regulatory role in multiple biological processes such as apoptosis, metabolism, inflammation, and tumorigenesis [35, 36]. Previous studies have indicated that MSC-derived could affect myocardial infarction via delivering miRNAs [37, 38]. However, large identifications on the efficacy of MSC

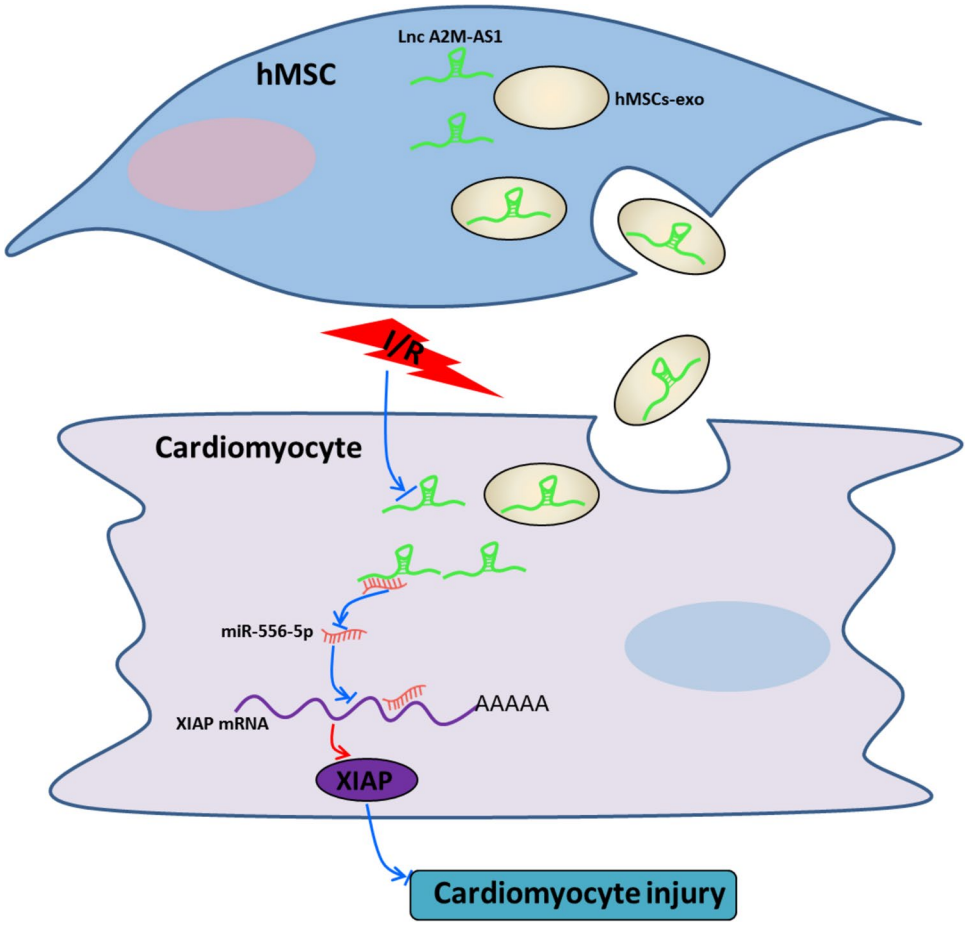

Fig. 8 A schematic of the working mechanism of Lnc A2M-AS1 delivery via MSC-derived exosomes in H/R-induced cardiomyocytes. Lnc A2M-AS1 delivery via MSC-derived exosomes suppressed H/R-induced cardiomyocyte injury via miR-556-5p/XIAP axis

exosome-based therapies with lncRNAs in myocardial injury has not been reported yet. Lnc A2M-AS1 was found to weaken H/R-induced apoptosis in cardiomyocytes [25], while its level in exosomes from hypoxic cardiomyocytes was decreased [28]. In this study, Lnc A2M-AS1 was discovered to be lowly expressed in AMI patients and H/R-induced cardiomyocytes. We then elevated the level of Lnc A2M-AS1 in MSC-derived exosomes; our results showed that exosomal Lnc A2M-AS1 attenuated H/R-induced injury in cardiomyocytes; importantly, Lnc A2M-AS1 reinforced the protective role of MSC-derived exosomes in H/R-damaged cardiomyocytes. The aforementioned findings demonstrated that Lnc A2M-AS1 delivery via MSC-derived exosomes protected cardiomyocytes against H/R-mediated injury, suggesting a novel insight into the MSC exosome–based therapy in myocardial I/R.

Increasing evidence has clarified that lncRNAs can act as miRNA sponges and protect he target mRNAs from repression [26, 27]. The present study verified that Lnc A2M-AS1 directly bound to miR-556-5p, and suppressed its expression in a targeted manner. Besides, we also validated that miR-556-5p targetedly inhibited XIAP expression; importantly, Lnc A2M-AS1 sponged miR-556-5p to relieve the suppression of miR-556-5p on XIAP expression. Thus, a Lnc A2M-AS1/miR-556-5p/XIAP feedback loop in cardiomyocytes was identified. Previous study showed that miR-556-5p was highly expressed in AMI patients [39]. XIAP belongs to the inhibitors of apoptosis (IAP) family, and negatively regulates cell apoptosis [40]. Lu's team displayed that ectopic up-regulation of XIAP impaired cell oxidative stress and survival in H/R-damaged cardiomyocytes [41]. Besides that, XIAP served as a target of miR-181a to reverse cardiomyocyte apoptosis induced by H/R [42]. In the current study, we demonstrated that miR-556-5p overexpression or XIAP knockdown attenuated the inhibitory functions of Lnc A2M-AS1, delivered by MSC-derived exosomes, in H/R-induced cardiomyocyte apoptotic and oxidative injury.

In conclusion, this work revealed that Lnc A2M-AS1 delivery via MSC-derived exosomes suppressed H/R-induced cardiomyocyte apoptosis, oxidative stress, and injury through miR-556-5p/XIAP axis (Fig. 8), opening a new avenue into the pathogenesis of myocardial I/R and the development of MSC exosome–based therapy for myocardial I/R.

Abbreviations *MSC*: mesenchymal stem cells; *I/R*: ischemia-reperfusion; *LncRNA*: long non-coding RNA; *A2M-AS1*: alpha-2-macroglobulin antisense RNA 1; *TEM*: transmission electron microscopy; *NTA*: nanoparticle tracking analysis; *H/R*: hypoxia/reoxygenation; *LDH*: lactate dehydrogenase; *MDA*: malondialdehyde; *SOD*: superoxide dismutase; *XIAP*: X-linked inhibitor of apoptosis protein; *AMI*: acute myocardial infarction; *CCK-8*: cell counting Kit-8; *GAPDH*: glyceraldehyde-3-phosphate dehydrogenase; *FITC*: fluorescein isothiocvanate; *PI*: propidium iodide; *Bcl-2*: B-cell lymphoma-2; *Bax*: Bcl-2-associated X protein; *qRT-PCR*: quantitative real-time polymerase chain reaction; *RIP*: RNA immunoprecipitation; *SD*: standard deviation; *MUT*: mutant; *WT*: wild-type; *siRNA*: small interfering RNA

Supplementary Information The online version contains supplementary material available at https://doi.org/10.1007/s10557-022-07339-7.

Author Contribution Hang Yu was responsible for drafting the manuscript. Hang Yu, Yuxiang Pan, and Mingming Dai contributed to the analysis and interpretation of data. Hang Yu, Xiaoqi Wang, and Haibo Chen contributed in the data collection. All authors read and approved the final manuscript.

Funding This work was supported by Natural Science Foundation of Hainan Province (No. 820MS143) and Medical and Health Research Projects in Hainan Province (No. 20A200364) and In-hospital Scientific Research and Cultivation Fund of the Second Affiliated Hospital of Hainan Medical College (The Second Affiliated Hospital of Haiyi Hospital (50)).

Declarations

All study participants provided their written informed consent for study participation, and study protocol was approved by the Ethics Committee of the Second Affiliated Hospital of Hainan Medical College in accordance with the Declaration of Helsinki.

Ethics Approval and Consent Participate Written informed consent was obtained from patients with approval by the Institutional Review Board in The Second Affiliated Hospital of Hainan Medical College.

Consent for Publication Not applicable.

Competing Interests The authors declare no competing interests.

References

1. Deng D, Liu L, Xu G, Gan J, Shen Y, Shi Y, Zhu R, Lin Y. Epidemiology and serum metabolic characteristics of acute myocardial infarction patients in chest pain centers. Iran J Public Health. 2018;47(7):1017–29.
2. Hausenloy DJ, Yellon DM. Myocardial ischemia-reperfusion injury: a neglected therapeutic target. J Clin Invest. 2013;123(1):92–100.
3. Prasad A, Stone GW, Holmes DR, Gersh B. Reperfusion injury, microvascular dysfunction, and cardioprotection: the "dark side" of reperfusion. Circulation. 2009;120(21):2105–12.
4. Kunecki M, Płazak W, Podolec P, Gołba KS. Effects of endogenous cardioprotective mechanisms on ischemia-reperfusion injury. Postepy Hig Med Dosw. 2017;71:20–31.
5. Ito H, Maruyama A, Iwakura K, Takiuchi S, Masuyama T, Hori M, Higashino Y, Fujii K, Minamino T. Clinical implications of the 'no reflow' phenomenon. A predictor of complications and left ventricular remodeling in reperfused anterior wall myocardial infarction. Circulation. 1996;93(2):223–8.
6. Ran X, Diao JX, Sun XG, Wang M, An H, Huang GQ, Zhao XS, Ma WX, Zhou FH, Yang YG, et al. Huangzhi oral liquid prevents arrhythmias by upregulating caspase-3 and apoptosis network proteins in myocardial ischemia-reperfusion injury in rats. Evid Based Complement Alternat Med. 2015;2015:518926.

7. Horwitz EM, Le Blanc K, Dominici M, Mueller I, Slaper-Cortenbach I, Marini FC, Deans RJ, Krause DS, Keating A. Clarification of the nomenclature for MSC: The International Society for Cellular Therapy position statement. Cytotherapy. 2005;7(5):393–5.
8. Samsonraj RM, Raghunath M, Nurcombe V, Hui JH, van Wijnen AJ, Cool SM. Concise review: multifaceted characterization of human mesenchymal stem cells for use in regenerative medicine. Stem Cells Transl Med. 2017;6(12):2173–85.
9. Szydlak R. Mesenchymal stem cells' homing and cardiac tissue repair. Acta Biochim Pol. 2019;66(4):483–9.
10. Sohni A, Verfaillie CM. Mesenchymal stem cells migration homing and tracking. Stem Cells Int. 2013;2013:130763.
11. Afzal MR, Samanta A, Shah ZI, Jeevanantham V, Abdel-Latif A, Zuba-Surma EK, Dawn B. Adult bone marrow cell therapy for ischemic heart disease: evidence and insights from randomized controlled trials. Circ Res. 2015;117(6):558–75.
12. Pedrosa M, Gomes J, Laranjeira P, Duarte C, Pedreiro S, Antunes B, Ribeiro T, Santos F, Martinho A, Fardilha M, et al. Immunomodulatory effect of human bone marrow-derived mesenchymal stromal/stem cells on peripheral blood T cells from rheumatoid arthritis patients. J Tissue Eng Regen Med. 2020;14(1):16–28.
13. Zhou R, Chen KK, Zhang J, Xiao B, Huang Z, Ju C, Sun J, Zhang F, Lv XB, Huang G. The decade of exosomal long RNA species: an emerging cancer antagonist. Mol Cancer. 2018;17(1):75.
14. Lugea A, Waldron RT. Exosome-Mediated Intercellular Communication Between Stellate Cells and Cancer Cells in Pancreatic Ductal Adenocarcinoma. Pancreas. 2017;46(1):1–4.
15. Roma-Rodrigues C, Fernandes AR, Baptista PV. Exosome in tumour microenvironment: overview of the crosstalk between normal and cancer cells. Biomed Res Int. 2014;2014:179486.
16. Milane L, Singh A, Mattheolabakis G, Suresh M, Amiji MM. Exosome mediated communication within the tumor microenvironment. J Control Release. 2015;219:278–94.
17. Kosaka N, Yoshioka Y, Fujita Y, Ochiya T. Versatile roles of extracellular vesicles in cancer. J Clin Invest. 2016;126(4):1163–72.
18. Zhou H, Wang B, Yang Y, Jia Q, Qi Z, Zhang A, Lv S, Zhang J. Exosomes in ischemic heart disease: novel carriers for bioinformation. Biomed Pharmacother. 2019;120:109451.
19. Chen GH, Xu J, Yang YJ. Exosomes: promising sacks for treating ischemic heart disease? Am J Phys Heart Circ Phys. 2017;313(3):H508–h523.
20. Liu L, Jin X, Hu CF, Li R, Zhou Z, Shen CX. Exosomes derived from mesenchymal stem cells rescue myocardial ischaemia/reperfusion injury by inducing cardiomyocyte autophagy via AMPK and Akt pathways. Cell Physiol Biochem Int J Exp Cell Physiol Biochem Pharmacol. 2017;43(1):52–68.
21. Arslan F, Lai RC, Smeets MB, Akeroyd L, Choo A, Aguor EN, Timmers L, van Rijen HV, Doevendans PA, Pasterkamp G, et al. Mesenchymal stem cell-derived exosomes increase ATP levels, decrease oxidative stress and activate PI3K/Akt pathway to enhance myocardial viability and prevent adverse remodeling after myocardial ischemia/reperfusion injury. Stem Cell Res. 2013;10(3):301–12.
22. Li Z, Zhang Y, Ding N, Zhao Y, Ye Z, Shen L, Yi H, Zhu Y. Inhibition of lncRNA XIST improves myocardial I/R injury by targeting miR-133a through inhibition of autophagy and regulation of SOCS2. Mol Ther Nucleic Acids. 2019;18:764–73.
23. Li X, Luo S, Zhang J, Yuan Y, Jiang W, Zhu H, Ding X, Zhan L, Wu H, Xie Y, et al. lncRNA H19 alleviated myocardial I/RI via suppressing miR-877-3p/Bcl-2-mediated mitochondrial apoptosis. Mol Ther Nucleic Acids. 2019;17:297–309.
24. Qiu L, Liu X. Identification of key genes involved in myocardial infarction. Eur J Med Res. 2019;24(1):22.
25. Song XL, Zhang FF, Wang WJ, Li XN, Dang Y, Li YX, Yang Q, Shi MJ, Qi XY. LncRNA A2M-AS1 lessens the injury of cardiomyocytes caused by hypoxia and reoxygenation via regulating IL1R2. Genes Genom. 2020;42(12):1431–41.
26. Chen S, Wang J. HAND2-AS1 inhibits invasion and metastasis of cervical cancer cells via microRNA-330-5p-mediated LDOC1. Cancer Cell Int. 2019;19:353.
27. Chen J, Lin Y, Jia Y, Xu T, Wu F, Jin Y. LncRNA HAND2-AS1 exerts anti-oncogenic effects on ovarian cancer via restoration of BCL2L11 as a sponge of microRNA-340-5p. J Cell Physiol. 2019;234(12):23421–36.
28. Wang L, Zhang J. Exosomal lncRNA AK139128 Derived from hypoxic cardiomyocytes promotes apoptosis and inhibits cell proliferation in cardiac fibroblasts. Int J Nanomedicine. 2020;15:3363–76.
29. Cooks T, Pateras IS, Jenkins LM, Patel KM, Robles AI, Morris J, Forshew T, Appella E, Gorgoulis VG, Harris CC. Mutant p53 cancers reprogram macrophages to tumor supporting macrophages via exosomal miR-1246. Nat Commun. 2018;9(1):771.
30. Gnecchi M, Danieli P, Malpasso G, Ciuffreda MC. Paracrine mechanisms of mesenchymal stem cells in tissue repair. Methods Mol Biol. 2016;1416:123–46.
31. Phinney DG, Prockop DJ. Concise review: mesenchymal stem/multipotent stromal cells: the state of transdifferentiation and modes of tissue repair--current views. Stem Cells. 2007;25(11):2896–902.
32. Martin-Rendon E, Sweeney D, Lu F, Girdlestone J, Navarrete C, Watt SM. 5-Azacytidine-treated human mesenchymal stem/progenitor cells derived from umbilical cord, cord blood and bone marrow do not generate cardiomyocytes in vitro at high frequencies. Vox Sang. 2008;95(2):137–48.
33. Zou L, Ma X, Wu B, Chen Y, Xie D, Peng C. Protective effect of bone marrow mesenchymal stem cell-derived exosomes on cardiomyoblast hypoxia-reperfusion injury through the miR-149/let-7c/Faslg axis. Free Radic Res. 2020;54(10):722–31.
34. Wang Y, Liang J, Xu J, Wang X, Zhang X, Wang W, Chen L, Yuan T. Circulating exosomes and exosomal lncRNA HIF1A-AS1 in atherosclerosis. Int J Clin Exp Pathol. 2017;10(8):8383–8.
35. Ma L, Bajic VB, Zhang Z. On the classification of long noncoding RNAs. RNA Biol. 2013;10(6):925–33.
36. Wu J, Zhao W, Wang Z, Xiang X, Zhang S, Liu L. Long non-coding RNA SNHG20 promotes the tumorigenesis of oral squamous cell carcinoma via targeting miR-197/LIN28 axis. J Cell Mol Med. 2019;23(1):680–8.
37. Zhu LP, Tian T, Wang JY, He JN, Chen T, Pan M, Xu L, Zhang HX, Qiu XT, Li CC, et al. Hypoxia-elicited mesenchymal stem cell-derived exosomes facilitates cardiac repair through miR-125b-mediated prevention of cell death in myocardial infarction. Theranostics. 2018;8(22):6163–77.
38. Peng Y, Zhao JL, Peng ZY, Xu WF, Yu GL. Exosomal miR-25-3p from mesenchymal stem cells alleviates myocardial infarction by targeting pro-apoptotic proteins and EZH2. Cell Death Dis. 2020;11(5):317.
39. Zhong Z, Wu H, Zhong W, Zhang Q, Yu Z. Expression profiling and bioinformatics analysis of circulating microRNAs in patients with acute myocardial infarction. J Clin Lab Anal. 2020;34(3):e23099.
40. Vucic D. XIAP at the crossroads of cell death and inflammation. Oncotarget. 2018;9(44):27319–20.

41. Lu M, Qin X, Yao J, Yang Y, Zhao M, Sun L. MiR-134-5p targeting XIAP modulates oxidative stress and apoptosis in cardiomyocytes under hypoxia/reperfusion-induced injury. IUBMB Life. 2020;72(10):2154–66.

42. Hao P, Cao X, Zhu Z, Gao C, Chen Y, Qi D. Effects of miR-181a targeting XIAP gene on apoptosis of cardiomyocytes induced by hypoxia/reoxygenation and its mechanism. J Cell Biochem. 2018.